

First-order spatial coherence of excitons in planar nanostructures: A k_{\parallel} -filtering effect

L. Mouchliadis and A. L. Ivanov

Department of Physics and Astronomy, Cardiff University, Queens Buildings, CF24 3AA Cardiff, United Kingdom

(Received 16 January 2008; revised manuscript received 15 May 2008; published 22 July 2008)

We propose and analyze a k_{\parallel} -filtering effect which gives rise to the drastic difference between the actual spatial coherence length of quasi-two-dimensional excitons or microcavity polaritons in planar nanostructures and that inferred from far-field optical measurements. The effect originates from conservation of the in-plane wave-vector k_{\parallel} in the optical decay of the particles in outgoing bulk photons. The k_{\parallel} -filtering effect explains the large coherence lengths recently observed for indirect excitons in coupled quantum wells but is less pronounced for microcavity polaritons at low temperatures, $T \lesssim 10$ K.

DOI: 10.1103/PhysRevB.78.033306

PACS number(s): 78.67.De, 71.35.-y, 42.50.Ar

Long-range spatial coherence is a fingerprint of well-developed Bose-Einstein (BE) statistics. Measurements of the first-order spatial coherence function $g^{(1)}$ and the coherence length ξ have allowed visualization of the BE condensation transition in a trapped Bose gas of Rb atoms.¹ There are several recent reports on the observation of long-range spatial optical coherence in a low-temperature quasi-two-dimensional (quasi-2D) system of microcavity (MC) polaritons^{2,3} and indirect excitons.⁴⁻⁷ In this case, the resonant optical decay of MC polaritons or quantum well (QW) excitons in bulk photon modes allows mapping of the in-plane coherence function $g^{(1)}$ of the particles by measuring the optical coherence function $\tilde{g}^{(1)}$ of the emitted photons. It is commonly assumed that the coherence length of QW excitons (MC polaritons), $\xi_x(\xi_p)$, associated with $g^{(1)}$, is identical to that, ξ_γ , of the optical coherence function $\tilde{g}^{(1)}$.

In this Brief Report, we report a k_{\parallel} -filtering effect, which can strongly influence the optical coherence function $\tilde{g}^{(1)}$ measured from a planar nanostructure, and calculate $g^{(1)}$ and $\tilde{g}^{(1)}$ for QW excitons and MC polaritons. For QW excitons, the k_{\parallel} -filtering effect tremendously increases the optical coherence length ξ_γ , leading to $\xi_\gamma \gg \xi_x$, and can naturally explain the micron coherence lengths observed for indirect excitons and attributed to spontaneously developed coherence. The effect is less pronounced for MC polaritons, still with $\xi_\gamma \gtrsim \xi_p$.

The k_{\parallel} -filtering effect stems from the energy and in-plane momentum conservation in the resonant conversion “quasi-2D QW exciton (MC polariton) \rightarrow outgoing bulk photon.” For a QW structure surrounded by thick coplanar barrier layers, the case illustrated in Fig. 1, only low-energy optically active excitons from the radiative zone $k_{\parallel} \leq k_0 = (\sqrt{\epsilon_b}/c)\omega_0$, with ϵ_b the dielectric constant of barrier layers and $\hbar\omega_0$ the exciton energy at $k_{\parallel}=0$, are bright, i.e., can emit far-field light.⁸⁻¹¹ In a far-field optical experiment with detection angle 2α [see Fig. 1(b)], the fraction of QW excitons which contribute to the optical signal is drastically further reduced to the wave-vector band Δk_{\parallel} given by $0 \leq k_{\parallel} \leq k_{\parallel}^{(\alpha)} = (k_0/\sqrt{\epsilon_b})\sin \alpha \ll k_0$. The α -dependent narrowing of the detected states results in an effective broadening of the first-order spatial coherence function $\tilde{g}^{(1)}$. In addition, the sharp cutoff of the detected states at $k_{\parallel}=k_{\parallel}^{(\alpha)}$ yields an unusual oscillatory behavior of $\tilde{g}^{(1)}$. The k_{\parallel} -filtering effect has no analog in optics of bulk excitons or polaritons.

The first-order spatial coherence function $g^{(1)}$ (Refs. 12 and 13) of quantum well excitons, at a fixed time, is given by $g^{(1)}(\mathbf{r}'_{\parallel}, \mathbf{r}''_{\parallel}) = G^{(1)}(\mathbf{r}'_{\parallel}, \mathbf{r}''_{\parallel}) / [G^{(1)}(\mathbf{r}'_{\parallel}, \mathbf{r}'_{\parallel})G^{(1)}(\mathbf{r}''_{\parallel}, \mathbf{r}''_{\parallel})]^{1/2}$, with $G^{(1)}(\mathbf{r}'_{\parallel}, \mathbf{r}''_{\parallel}) = \langle \hat{\Psi}^\dagger(\mathbf{r}'_{\parallel}) \hat{\Psi}(\mathbf{r}''_{\parallel}) \rangle$, where $\hat{\Psi}(\mathbf{r}'_{\parallel}) = (1/\sqrt{S}) \sum_{\mathbf{k}_{\parallel}} e^{i\mathbf{k}_{\parallel} \cdot \mathbf{r}'_{\parallel}} B_{\mathbf{k}_{\parallel}}$, \mathbf{r}'_{\parallel} is the in-plane coordinate, S is the area, and $B_{\mathbf{k}_{\parallel}}$ is the exciton operator. Thus for isotropically distributed QW excitons one receives

$$g^{(1)} = g^{(1)}(r_{\parallel}) = \frac{1}{2\pi n_{2d}} \int_0^{\infty} J_0(k_{\parallel} r_{\parallel}) n_{k_{\parallel}} k_{\parallel} dk_{\parallel}, \quad (1)$$

where $r_{\parallel} = |\mathbf{r}'_{\parallel} - \mathbf{r}''_{\parallel}|$, n_{2d} is the concentration of particles, $n_{\mathbf{k}_{\parallel}} = \langle B_{\mathbf{k}_{\parallel}}^\dagger B_{\mathbf{k}_{\parallel}} \rangle$ is the occupation number, and J_0 is the zeroth-order Bessel function of the first kind. For a classical gas of QW excitons at thermal equilibrium, Eq. (1), with $n_{\mathbf{k}_{\parallel}}$ given by the Maxwell-Boltzmann (MB) distribution function $n_{\mathbf{k}_{\parallel}}^{\text{MB}}$, yields the well-known result,^{3,14}

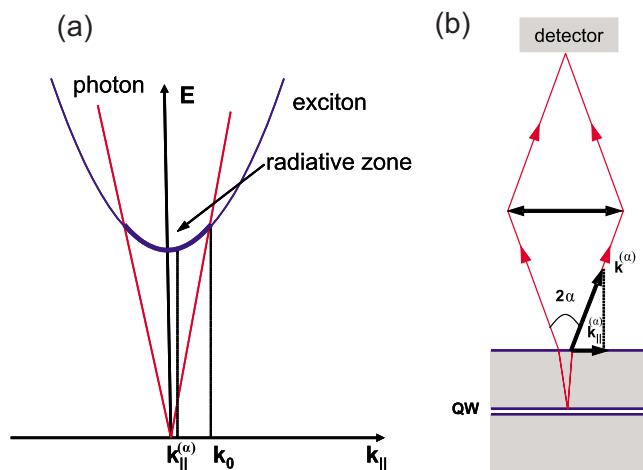


FIG. 1. (Color online) Schematic of the k_{\parallel} -filtering effect. (a) The exciton and photon dispersions. Only low-energy QW excitons from the radiative zone $k_{\parallel} \leq k_0$ can emit outgoing bulk photons. (b) A far-field optical experiment with detection angle 2α : a small fraction of QW excitons with $|k_{\parallel}| \leq k_{\parallel}^{(\alpha)} = (k_0/\sqrt{\epsilon_b})\sin \alpha$ contributes to the optical signal.

$$g^{(1)} = g_{\text{cl}}^{(1)}(r_{\parallel}) = e^{-\pi r_{\parallel}^2 / \lambda_{\text{dB}}^2}, \quad (2)$$

where the thermal de Broglie wavelength is given by $\lambda_{\text{dB}} = [(2\pi\hbar^2)/(M_x k_B T)]^{1/2}$, with T the temperature and M_x the exciton in-plane translational mass. For helium temperatures, one estimates from Eq. (2) the coherence length of MB-distributed indirect excitons in GaAs coupled QWs as $\xi_x \sim \lambda_{\text{dB}} \sim 0.1 \mu\text{m}$.

Compared with Eq. (1), the spatial coherence function $\bar{g}^{(1)}$ of photons emitted by QW excitons is given by

$$\bar{g}^{(1)}(r_{\parallel}) = \frac{\int_0^{\infty} G_f(k_{\parallel}) J_0(k_{\parallel} r_{\parallel}) n_{k_{\parallel}} k_{\parallel} dk_{\parallel}}{\int_0^{\infty} G_f(k_{\parallel}) n_{k_{\parallel}} k_{\parallel} dk_{\parallel}}, \quad (3)$$

where $G_f = \Theta(k_{\parallel}^{(\alpha)} - k_{\parallel}) \Gamma_{x-\gamma}(k_{\parallel})$ is the k_{\parallel} -filtering function, with $\Theta(x)$ the step function and $\Gamma_{x-\gamma}(k_{\parallel})$ the efficiency of the resonant conversion of a QW exciton in an outgoing bulk photon. The function G_f reduces the integration limits on the right-hand side (rhs) of Eq. (3) to the narrow band $\Delta k_{\parallel} = [0, k_{\parallel}^{(\alpha)}]$ and describes the k_{\parallel} -filtering effect in high-quality planar nanostructures. If both the function $\Gamma_{x-\gamma}(k_{\parallel})$ and the occupation number $n_{k_{\parallel}}$ do not change significantly in the narrow band Δk_{\parallel} , Eq. (3) yields

$$\bar{g}^{(1)} = \bar{g}_f^{(1)}(r_{\parallel}) = 2J_1(k_{\parallel}^{(\alpha)} r_{\parallel}) / (k_{\parallel}^{(\alpha)} r_{\parallel}), \quad (4)$$

where J_1 is the first-order Bessel function of the first kind. From Eq. (4) one concludes that the optical coherence length ξ_{γ} , evaluated as the half width at half maximum of $\bar{g}^{(1)} = \bar{g}_f^{(1)}(r_{\parallel})$, is given by

$$4J_1(k_{\parallel}^{(\alpha)} \xi_{\gamma}) = k_{\parallel}^{(\alpha)} \xi_{\gamma} \rightarrow k_{\parallel}^{(\alpha)} \xi_{\gamma} \approx 2.215. \quad (5)$$

Equations (4) and (5) illustrate the net k_{\parallel} -filtering effect in the absence of instrumental aberrations: $\xi_{\gamma} \propto 1/k_{\parallel}^{(\alpha)} \propto 1/\sin \alpha$ strongly increases with decreasing aperture angle 2α . Below we analyze in more detail the exciton function $g^{(1)}$ against the optical $\bar{g}^{(1)}$, assuming no phase transition to a collective (superfluid) state.

First-order spatial coherence of noninteracting quasi-2D bosons (excitons) in equilibrium. In this case, the chemical potential μ_{2d} is given by $\mu_{2d}^{(0)} = k_B T \ln(1 - e^{-T_0/T})$, with $k_B T_0 = (2\pi/g)(\hbar^2/M_x) n_{2d}$ the quantum degeneracy temperature where g is the spin degeneracy factor of bosons ($g=4$ for indirect excitons). By substituting $n_{k_{\parallel}} = n_{k_{\parallel}}^{\text{BE}}$ into Eq. (1), where $n_{k_{\parallel}}^{\text{BE}}$ is the Bose-Einstein occupation number, one receives

$$g^{(1)} = g_{\text{nit}}^{(1)}(r_{\parallel}) = \frac{T}{T_0} g_1(1 - e^{-T_0/T}, e^{-\pi r_{\parallel}^2 / \lambda_{\text{dB}}^2}) \\ = \frac{T}{T_0} \sum_{n=1}^{\infty} \frac{(1 - e^{-T_0/T})^n}{n} e^{-\pi r_{\parallel}^2 / n \lambda_{\text{dB}}^2}. \quad (6)$$

Here, the generalized Bose function¹⁴ $g_{\nu}(x, y)$ with $\nu=1$ is defined as $g_{\nu}(x, y) = \sum_{k=1}^{\infty} (x^k y^{1/k}) / k^{\nu}$.

For distances $r_{\parallel} \geq r_{\parallel}^{(q)} = \lambda_{\text{dB}} [- (2/\pi) \ln(1 - e^{-T_0/T})]^{1/2}$ Eq. (6) reduces to the quantum limit when the sum on the rhs cannot be approximated by the first term,

$$g^{(1)}(r_{\parallel} \geq r_{\parallel}^{(q)}) \approx 2 \frac{T}{T_0} K_0 \left(\frac{r_{\parallel}}{r_0} \right), \quad (7)$$

where K_0 is the modified Bessel function of the second kind and $r_0 = \lambda_{\text{dB}} [-4\pi \ln(1 - e^{-T_0/T})]^{1/2}$. For $r_{\parallel} \geq r_0 \geq r_{\parallel}^{(q)}$, Eq. (7) reduces further to

$$g^{(1)} = g_q^{(1)}(r_{\parallel} \geq r_0) = \sqrt{2\pi} \frac{T}{T_0} \sqrt{\frac{r_0}{r_{\parallel}}} e^{-r_{\parallel}/r_0}. \quad (8)$$

For temperatures $T \gg T_0$, the spatial coherence function is well approximated by Eq. (2), and the quantum corrections given by Eqs. (7) and (8) refer to large $r_{\parallel} \geq r_{\parallel}^{(q)} \approx \lambda_{\text{dB}} \sqrt{(2/\pi) \ln(T/T_0)} \gg \lambda_{\text{dB}}$ and, therefore, to very small values of $g^{(1)}$. For $T \leq T_0$, when BE statistics is well developed, Eqs. (7) and (8) are valid for distances larger than $r_{\parallel}^{(q)} \approx \lambda_{\text{dB}} \sqrt{(2/\pi) e^{-T_0/2T}} \ll \lambda_{\text{dB}}$, so that $g^{(1)}$ is well approximated by $g_q^{(1)}$ for any r_{\parallel} . The quantum statistical effects, which are included in Eq. (7) through $T_0 \propto \hbar^2$, considerably increase the correlation length ξ_x , giving rise to $\xi_x \approx [\lambda_{\text{dB}} / (2\sqrt{\pi})] e^{T_0/2T}$ for $T \leq T_0$ (see Fig. 2).

The coherence function $g^{(1)}$ of weakly interacting thermal QW excitons. For circularly polarized excitons in single QWs, the case relevant to MC polaritons, the repulsive interaction between the particles is well approximated by a contact potential $U_{\text{SQW}} = (u_0/2) \delta(\mathbf{r}_{\parallel})$, with $u_0 = u_0^{\text{SQW}} > 0$. In this case, the mean-field Hartree-Fock (HF) interaction only shifts the chemical potential, $\mu_{2d} = \tilde{\mu}_{2d}^{(0)} = \mu_{2d}^{(0)} + u_0 n_{2d}$, leaving unchanged Eqs. (6)–(8).

For indirect excitons in coupled QWs, the mid-range dipole-dipole repulsive interaction U_{CQW} of the particles cannot be generally approximated by a contact potential. Following Ref. 15, we use the two-parametric model potential $U_{\text{CQW}}(r_{\parallel}) = [(\sqrt{\pi} u_0 w) / r_{\parallel}^3] (1 - e^{-r_{\parallel}^2/w^2})$, with parameters $u_0 = u_0^{\text{CQW}} \approx 4\pi(e^2/\epsilon_b) d_z$ (Refs. 16 and 17) and $w \approx a_x^{(2d)}$, where d_z is the distance between coupled quantum wells and $a_x^{(2d)}$ is the radius of an indirect exciton. The model potential reproduces $1/r_{\parallel}^3$ behavior at $r_{\parallel} \gtrsim a_x^{(2d)}$ and $1/r_{\parallel}$ Coulomb repulsive potential at $r_{\parallel} \lesssim a_x^{(2d)}$. The self-consistent HF analysis¹⁸ of the Hamiltonian $H_x = \sum_{\mathbf{p}_{\parallel}} [p_{\parallel}^2 / (2M_x)] B_{\mathbf{p}_{\parallel}}^{\dagger} B_{\mathbf{p}_{\parallel}} + 1 / (2S) \sum_{\mathbf{p}_{\parallel}, \mathbf{q}_{\parallel}} U_{\text{CQW}}(\mathbf{q}_{\parallel}) B_{\mathbf{p}_{\parallel}}^{\dagger} B_{\mathbf{p}_{\parallel} + \mathbf{q}_{\parallel}}^{\dagger} B_{\mathbf{p}_{\parallel} - \mathbf{q}_{\parallel}} B_{\mathbf{p}_{\parallel}}$ yields the n_{2d} - and T -dependent change in the in-plane translational mass M_x . In this case, μ_{2d} is

$$\mu_{2d} = \tilde{\mu}_{2d}^{(0)} + \frac{u_0}{2(\lambda_{\text{dB}}^*)^2} \left\{ \frac{T_0^*}{T} + \sqrt{\pi} \frac{w}{\lambda_{\text{dB}}^*} \left[\frac{\sqrt{\pi} w}{2 \lambda_{\text{dB}}^*} \text{Li}_2(F) - \text{Li}_{3/2}(F) \right] \right\}, \quad (9)$$

where, together with Eq. (6), both the de Broglie wavelength λ_{dB}^* and the degeneracy temperature T_0^* are changed according to $M_x \rightarrow M_x^*$, $F = 1 - e^{-T_0^*/T}$, and $\text{Li}_{\nu}(x) = \sum_{k=1}^{\infty} x^k / k^{\nu}$ is the polylogarithm. The particle mass M_x^* renormalized by the dipole-dipole interaction is given as a single solution of the transcendental equation,

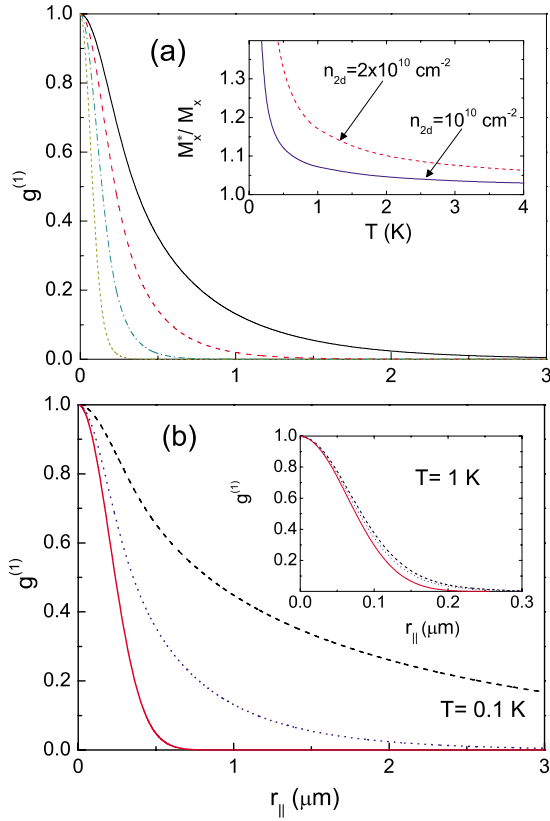


FIG. 2. (Color online) (a) The first-order spatial coherence function $g^{(1)} = g_{\text{ind}}^{(1)}(r_{\parallel})$ of indirect excitons in a GaAs coupled QW structure with $d_z = 11.5$ nm and $w = 15$ nm; $n_{2d} = 10^{10}$ cm $^{-2}$ and $T = 1$ K (dotted line), 0.4 K (dash-dotted line), 0.2 K (dashed line), and 0.1 K (solid line). Inset: the renormalized mass M_x^* against temperature T , calculated with Eq. (10). (b) $g_{\text{ind}}^{(1)} = g_{\text{ind}}^{(1)}(r_{\parallel})$ (solid line), $g_{\text{nint}}^{(1)} = g_{\text{nint}}^{(1)}(r_{\parallel})$ (dashed line), and $g_{\text{cl}}^{(1)} = g_{\text{cl}}^{(1)}(r_{\parallel})$ (dotted line): $n_{2d} = 10^{10}$ cm $^{-2}$ and $T = 0.1$ K. Inset: the same functions evaluated for $n_{2d} = 10^{10}$ cm $^{-2}$ and $T = 1$ K.

$$\frac{1}{M_x^*} = \frac{1}{M_x} + \frac{u_0 w}{8\sqrt{\pi}\hbar^2\lambda_{\text{dB}}^*} \left[\sqrt{\pi} \frac{w}{\lambda_{\text{dB}}^*} \frac{T_0^*}{T} - \text{Li}_{1/2}(F) \right]. \quad (10)$$

In Fig. 2(a) we plot $g^{(1)} = g_{\text{ind}}^{(1)}(r_{\parallel})$ evaluated numerically by using Eqs. (6), (9), and (10) for indirect excitons in a GaAs coupled QW structure. In Fig. 2(b), the coherence function $g_{\text{ind}}^{(1)}$ is compared with $g_{\text{cl}}^{(1)}$ evaluated with Eq. (2) and $g_{\text{nint}}^{(1)}$ calculated with Eq. (6) for noninteracting excitons. The main result is that the dipole-dipole repulsive interaction induces an increase in the translational mass [see the inset of Fig. 2(a)] and, therefore, decreases the coherence length ξ_x compared to that of noninteracting particles [see also Fig. 3(a)]. The effect, however, becomes pronounced only at temperatures well below 1 K. For $T = 1$ K all three correlation functions, $g_{\text{ind}}^{(1)}$, $g_{\text{cl}}^{(1)}$, and $g_{\text{nint}}^{(1)}$, nearly coincide, as is clearly seen in the inset of Fig. 2(b). In other words, for $n_{2d} = 10^{10}$ cm $^{-2}$ and $T = 1.5$ K, which are relevant to the experiments,⁴⁻⁷ the quantum limit, i.e., $g^{(1)} = g_q^{(1)}$ given by Eq. (8), cannot build up: One estimates $T_0 \approx T_0^* \approx 0.65$ K and $n_{k_{\parallel}=0}^{\text{BE}} \approx 0.54 < 1$, so that BE statistics is rather weakly developed to influence the coherence length ξ_x .

The given description of $g^{(1)}$ refers to temperatures above

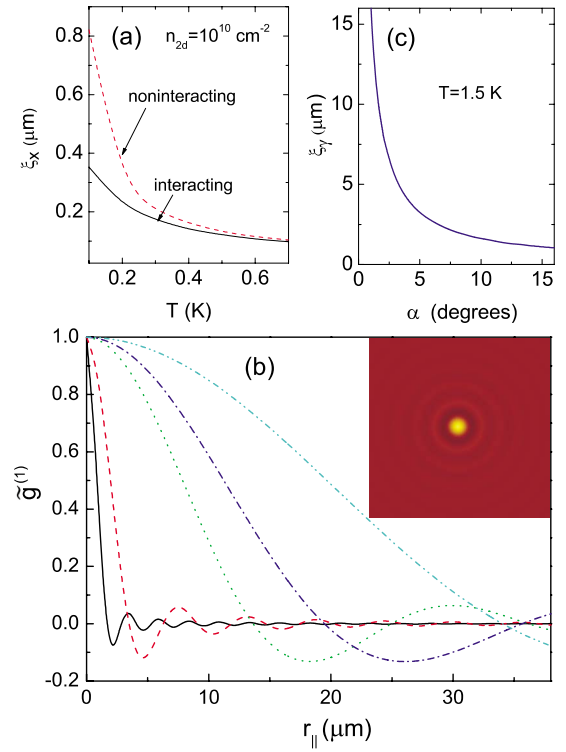


FIG. 3. (Color online) (a) The dependence of the correlation length ξ_x against temperature T , calculated for noninteracting (dashed line) and dipole-dipole interacting (solid line) indirect excitons. (b) The k_{\parallel} -filtering effect: $\tilde{g}^{(1)} = \tilde{g}^{(1)}(r_{\parallel})$ evaluated for $\alpha = 18.9^\circ$ (solid line), 8.3° (dashed line), 2.1° (dotted line), 1.4° (dash-dotted line), and 0.8° (dash-double-dotted line). Inset: the real-space 2D image of $\tilde{g}^{(1)}$. (c) The coherence length ξ_γ against the aperture angle 2α .

T_0 , i.e., when classical or weakly developed BE statistics are realized, and to a quantum gas of indirect excitons at $T \leq T_0$, but still above the phase transition temperature. In all these cases the correlation function for a quasi-2D system of weakly interacting excitons is universally given by Eq. (6).

The optical spatial coherence function $\tilde{g}^{(1)}$ of indirect excitons. In order to explain the experiments,⁴⁻⁷ which demonstrate a coherence length ξ_γ much larger than $\xi_x \sim 0.1$ μm , we implement the concept of k_{\parallel} -filtering. In this case, $\tilde{g}^{(1)} = \tilde{g}_{\text{ind}}^{(1)}(r_{\parallel})$ is given by Eq. (3) with the efficiency of the “indirect exciton \rightarrow bulk photon” conversion $\Gamma_{\text{ind}}^{\chi-\gamma} = (2k_0^2 - k_{\parallel}^2) / [k_0(k_0^2 - k_{\parallel}^2)^{1/2}]$.^{8-10,19} In Fig. 3(b), we plot $\tilde{g}_{\text{ind}}^{(1)}$ calculated for various aperture angles, $2^\circ \leq 2\alpha \leq 40^\circ$. The dependence $\tilde{g}^{(1)} = \tilde{g}_{\text{ind}}^{(1)}(r_{\parallel})$ is well approximated by Eq. (4). The above approximation of $\tilde{g}^{(1)}$ by the “device function” $\tilde{g}_f^{(1)}$ is valid when $n_{k_{\parallel}}^{\text{BE}} = n_{E=\hbar^2 k_{\parallel}^2 / 2M_x}$ is nearly constant in the rather narrow energy interval $0 \leq E \leq E^{(\alpha)}$, i.e., when $E^{(\alpha)} = (\hbar k_{\parallel}^{(\alpha)})^2 / 2M_x \ll k_B T e^{-T_0/T}$. For indirect excitons, this inequality with T_0 replaced by T_0^* is definitely held for $n_{2d} \sim 10^{10}$ cm $^{-2}$ and $T \sim 1$ K (e.g., for $\alpha = 20^\circ$ the cutoff energy $E^{(\alpha)}$ is only 1.2 μeV). Thus the k_{\parallel} -filtering effect yields the correlation length $\xi_\gamma \approx 2.215\sqrt{\epsilon_b} / (k_0 \sin \alpha)$, with $k_0 \approx 2.8 \times 10^5$ cm $^{-1}$, according to Eq. (5). As a result, ξ_γ is intrinsically scaled by the photon wavelength, i.e., is in the micron length scale [see Fig. 3(c), where ξ_γ is plotted against the angle α].

Compared to standard interference patterns in Young's double-slit experiment, with visibility contrast determined by $\tilde{g}^{(1)}$, the oscillatory behavior of the optical coherence function $\tilde{g}^{(1)} = \tilde{g}^{(1)}(r_{\parallel})$ is rather unusual [see Eq. (4) and Fig. 3(b)]. This is a signature of the k_{\parallel} -filtering effect: The k_{\parallel} -filtering function $G_f \propto \Theta(k_{\parallel}^{(\alpha)} - k_{\parallel})$ gives a sharp cutoff at $k_{\parallel} = k_{\parallel}^{(\alpha)}$ in the integrals of Eq. (3) that results in oscillations of $\tilde{g}^{(1)}(r_{\parallel})$. In some aspects, the effect is similar to Friedel oscillations in a Fermi liquid, with $\hbar k_{\parallel}^{(\alpha)}$ akin to the Fermi momentum.

The coherence function $\tilde{g}^{(1)}$ of MC polaritons. In this case, the "MC polariton \rightarrow bulk photon" conversion function in Eq. (3) is $\Gamma_{x-\gamma} = \Psi(k_{\parallel}) / \tau_{\gamma}(k_{\parallel})$, with Ψ ($0 \leq \Psi \leq 1$) the photon component along a MC polariton branch and τ_{γ} the radiative (escape) lifetime of a MC photon. In Fig. 4, $g^{(1)} = g_{\text{MC}}^{(1)}(r_{\parallel})$ calculated with Eq. (6) for circularly polarized MC polaritons is compared with $\tilde{g}^{(1)} = \tilde{g}_{\text{MC}}^{(1)}(r_{\parallel})$ evaluated with Eq. (3). According to the experiments,^{2,3} we assume the BE distribution of MC polaritons along the lower polariton branch which is taken in the parabolic approximation with an effective in-plane mass $M_{\text{MC}}^{\text{lb}}$. Compared to the case of QW excitons, the difference between $g_{\text{MC}}^{(1)}$ and $\tilde{g}_{\text{MC}}^{(1)}$ is much smaller, still giving $\xi_{\gamma} > \xi_p$. This is because the cutoff energy $E^{(\alpha)}$ in the k_{\parallel} -filtering effect is much larger than that relevant to QW excitons, due to $M_{\text{MC}}^{\text{lb}} \ll M_x$. If $k_B T \ll E^{(\alpha)} \sim 1$ meV, $g_{\text{MC}}^{(1)}$ and $\tilde{g}_{\text{MC}}^{(1)}$ nearly coincide (see Fig. 4).

We qualitatively explain a sharp increase in the coherence length with decreasing temperature, found in the experiments with coupled QWs,⁴⁻⁷ by combining the k_{\parallel} -filtering effect with screening of disorder by dipole-dipole interacting indirect excitons.¹⁷ In high-quality GaAs coupled QWs the screening process effectively develops at $T \lesssim 5$ K, giving

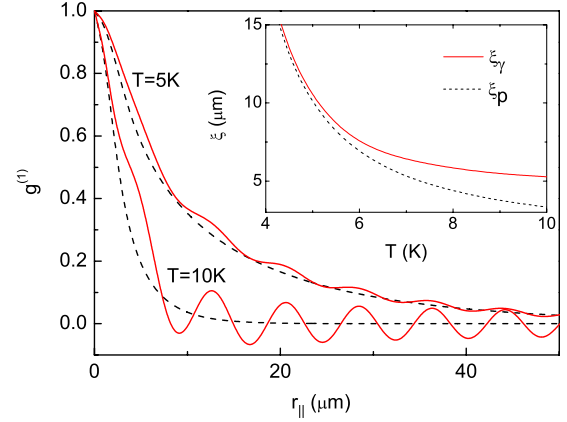


FIG. 4. (Color online) The MC polariton coherence function $g^{(1)} = g_{\text{MC}}^{(1)}(r_{\parallel})$ (dashed lines) against that of emitted photons, $\tilde{g}^{(1)} = \tilde{g}_{\text{MC}}^{(1)}(r_{\parallel})$ (solid lines). Inset: the coherence lengths ξ_p and ξ_{γ} versus temperature T . The calculations, which model the experiments (Ref. 3) refer to a GaAs microcavity with positive detuning $\delta = 7$ meV and Rabi splitting $\Omega_{\text{MC}} = 4$ meV. The density of MC polaritons $n_{2d} = 10^8$ cm $^{-2}$ and the aperture half-angle $\alpha = 16.7^\circ$, so that $T_0 = 27.6$ K and $E^{(\alpha)} = 0.96$ meV.

rise to a well-defined single-particle momentum $\hbar k_{\parallel}$, as has been observed, e.g., in the experiments.^{20,21} Thus the large correlation length $\xi = \xi_{\gamma} \sim 1$ μm can naturally be explained by the k_{\parallel} -filtering effect and cannot be interpreted as a signature of BE condensation in a system of indirect excitons.

We appreciate valuable discussions with L. V. Butov.

- ¹I. Bloch, T. W. Hänsch, and T. Esslinger, *Nature (London)* **403**, 166 (2000).
- ²J. Kasprzak, M. Richard, S. Kundermann, A. Baas, P. Jeambrun, J. M. J. Keeling, F. M. Marchetti, M. H. Szymańska, R. André, J. L. Staehli, V. Savona, P. B. Littlewood, B. Deveaud, and Le Si Dang, *Nature (London)* **443**, 409 (2006).
- ³H. Deng, G. S. Solomon, R. Hey, K. H. Ploog, and Y. Yamamoto, *Phys. Rev. Lett.* **99**, 126403 (2007).
- ⁴S. Yang, A. T. Hammack, M. M. Fogler, L. V. Butov, and A. C. Gossard, *Phys. Rev. Lett.* **97**, 187402 (2006).
- ⁵A. V. Gorbunov and V. B. Timofeev, *Pis'ma Zh. Eksp. Teor. Fiz.* **84**, 390 (2006) [*JETP Lett.* **84**, 329 (2006)].
- ⁶L. V. Butov, *J. Phys.: Condens. Matter* **19**, 295202 (2007).
- ⁷V. B. Timofeev, in *Problems of Condensed Matter Physics*, edited by A. L. Ivanov and S. G. Tikhodeev (Oxford University Press, Oxford, 2008), pp. 258–284.
- ⁸E. Hanamura, *Phys. Rev. B* **38**, 1228 (1988).
- ⁹L. C. Andreani, F. Tassone, and F. Bassani, *Solid State Commun.* **77**, 641 (1991).
- ¹⁰D. S. Citrin, *Phys. Rev. B* **47**, 3832 (1993).
- ¹¹C. Klingshirn, *Semiconductor Optics*, 3rd ed. (Springer, Berlin, 2007), Sec. 23.4.

- ¹²R. J. Glauber, in *Quantum Optics and Electronics*, edited by C. DeWitt, A. Blandin, and C. Cohen-Tannoudji (Gordon and Breach, New York, 1965).
- ¹³M. O. Scully and M. S. Zubairy, *Quantum Optics* (Cambridge University Press, Cambridge, 1997).
- ¹⁴M. Naraschewski and R. J. Glauber, *Phys. Rev. A* **59**, 4595 (1999).
- ¹⁵D. M. Kachintsev and S. E. Ulloa, *Phys. Rev. B* **50**, 8715 (1994).
- ¹⁶L. V. Butov, *J. Phys.: Condens. Matter* **16**, R1577 (2004).
- ¹⁷A. L. Ivanov, *Europhys. Lett.* **59**, 586 (2002).
- ¹⁸A. L. Fetter and J. D. Walecka, *Quantum Theory of Many-Particle Systems* (McGraw-Hill, New York, 1971).
- ¹⁹A. L. Ivanov, P. B. Littlewood, and H. Haug, *Phys. Rev. B* **59**, 5032 (1999).
- ²⁰A. Parlangeli, P. C. M. Christianen, J. C. Maan, I. V. Tokatly, C. B. Soerensen, and P. E. Lindelof, *Phys. Rev. B* **62**, 15323 (2000).
- ²¹L. V. Butov, A. L. Ivanov, A. Imamoglu, P. B. Littlewood, A. A. Shashkin, V. T. Dolgoplov, K. L. Campman, and A. C. Gossard, *Phys. Rev. Lett.* **86**, 5608 (2001).